ORGANIC
LETTERS

2012
Vol. 14, No. 17
4382–4385

Novel Butterfly-Shaped Fused Heteroacenes: Synthesis, Properties, and Device Performance of Solution-Processed Field-Effect Transistors

Weifeng Zhang,[†] Xiangnan Sun,[†] Pingfang Xia,[‡] Jianyao Huang,[†] Gui Yu,[*,†]
Man Shing Wong,[*,‡] Yunqi Liu,[*,†] and Daoben Zhu[†]

Beijing National Laboratory for Molecular Sciences, Institute of Chemistry, Chinese Academy of Sciences, Beijing 100190, P. R. China, and Institute of Molecular Functional Materials & Department of Chemistry & Centre for Advanced Luminescence Materials, Hong Kong Baptist University, Kowloon Tong, Hong Kong SAR, P. R. China

yugui@iccas.ac.cn; liuyq@iccas.ac.cn; mswong@hkbu.edu.hk

Received July 6, 2012

ABSTRACT

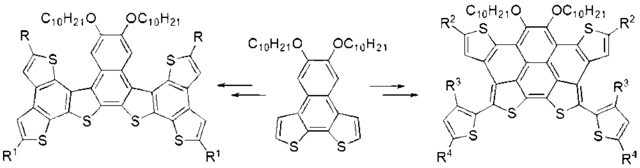

1 ($R = R^1 = C_6H_{13}$)
2 ($R = H, R^1 = Br$)
3 ($R = R^1 = H$)

4 ($R^2 = R^3 = H, R^4 = Br$)
5 ($R^2 = R^3 = R^4 = Br$)
6 ($R^2 = R^3 = R^4 = H$)

Two tetrabrominated intermediates obtained by bromination of naphthodithiophene in different solvents were used to construct novel highly π-extended butterfly-shaped heteroarenes 1–6, containing either an 8- or 10-fused ring. The solution-processed organic field-effect transistors based on compound 1 exhibited promising device performance with a hole mobility of 0.072 cm^2 V^{-1} s^{-1} and a current on/off ratio of 10^6 under ambient atmosphere.

Organic field-effect transistors (OFETs) have attracted much interest because of their potential applications in large area and flexible electronics.[1] Organic semiconductors are an important constituent of the OFET devices and determine their device performance. Many novel organic semiconductors have been designed and synthesized, such as linear,[2] star-shaped,[3] X-shaped,[4] and butterfly-shaped molecules[5] and π-conjugated polymers,[6] and some of them have achieved mobilities as high as that of amorphous silicon. However, exploring new organic semiconductors with excellent device performance and easily processable properties and setting up facile and effective synthetic methodology are still significant challenges.[7]

[†] Institute of Chemistry.
[‡] Hong Kong Baptist University.

(1) (a) Thompson, B.; Fréchet, J. *Angew. Chem., Int. Ed.* **2008**, *47*, 58. (b) Kido, J.; Kimura, M.; Nagai, K. *Science* **1995**, *267*, 1332. (c) Mas-Torrent, M.; Rovira, C. *Chem. Soc. Rev.* **2008**, *37*, 827. (d) Zaumseil, J.; Sirringhaus, H. *Chem. Rev.* **2007**, *107*, 1296.

(2) (a) Xiao, K.; Liu, Y.; Qi, T.; Zhang, W.; Wang, F.; Gao, J.; Qiu, W.; Ma, Y.; Cui, G.; Chen, S.; Zhan, X.; Yu, G.; Qin, J.; Hu, W.; Zhu, D. *J. Am. Chem. Soc.* **2005**, *127*, 13281. (b) Niimi, K.; Shinamura, S.; Osaka, I.; Miyazaki, E.; Takimiya, K. *J. Am. Chem. Soc.* **2011**, *133*, 8732. (c) Takimiya, K.; Shinamura, S.; Osaka, I.; Miyazaki, E. *Adv. Mater.* **2011**, *23*, 4347. (d) Gao, P.; Feng, X.; Yang, X.; Enkelmann, V.; Baumgarten, M.; Müllen, K. *J. Org. Chem.* **2008**, *73*, 9207.

(3) Kim, K.; Chi, Z.; Cho, M.; Jin, J.; Cho, M.; Kim, S.; Joo, J.; Choi, D. *Chem. Mater.* **2007**, *19*, 4925.

(4) (a) Jung, K.; Bae, S.; Kim, K.; Cho, M.; Lee, K.; Kim, Z.; Choi, D.; Lee, D.; Chung, D.; Park, C. *Chem. Commun.* **2009**, 5290. (b) Sun, X.; Zhou, Y.; Wu, W.; Liu, Y.; Tian, W.; Yu, G.; Qiu, W.; Chen, S.; Zhu, D. *J. Phys. Chem. B* **2006**, *110*, 7702.

(5) (a) Yin, J.; Zhou, Y.; Lei, T.; Pei, J. *Angew. Chem., Int. Ed.* **2011**, *50*, 6320. (b) Liu, W.; Zhou, Y.; Ma, M.; Cao, Y.; Wang, J.; Pei, J. *Org. Lett.* **2007**, *9*, 4187. (c) Zhang, S.; Guo, Y.; Zhang, Y.; Liu, R.; Li, Q.; Zhan, X.; Liu, Y.; Hu, W. *Chem. Commun.* **2010**, *46*, 2841. (d) Wang, J.; Zhou, Y.; Yan, J.; Ding, L.; Ma, Y.; Cao, Y.; Wang, J.; Pei, J. *Chem. Mater.* **2009**, *21*, 2595. (e) Zhou, Y.; Liu, W.; Ma, Y.; Wang, H.; Qi, L.; Cao, Y.; Wang, J.; Pei, J. *J. Am. Chem. Soc.* **2007**, *129*, 12386. (f) Zhou, Y.; Wang, L.; Wang, J.; Pei, J.; Cao, Y. *Adv. Mater.* **2008**, *20*, 3745.

(6) (a) Sirringhaus, H.; Kawase, T.; Friend, R.; Shimoda, T.; Inbasekaran, M.; Wu, W.; Woo, E. *Science* **2000**, *290*, 2123. (b) Yan, H.; Chen, Z.; Zheng, Y.; Newman, C.; Quinn, J.; Doltz, F.; Kestler, M.; Facchetti, A. *Nature* **2009**, *457*, 679. (c) Chen, H.; Hou, J.; Zhang, S.; Liang, Y.; Yang, G.; Yang, Y.; Yu, L.; Wu, Y.; Li, G. *Nat. Photonics* **2009**, *3*, 649.

10.1021/ol301852m

Heteroacenes are an important class of semiconductors, such as 2,7-diphenyl[1]benzothieno[3,2-*b*]benzothiophene and dinaphtho-[2,3-*b*:2′,3′-*f*]thieno[3,2-*b*]thiophene. These materials were used to fabricate high-performance OFET devices affording mobilities in the range 1.0–3.9 cm^2 V^{-1} s^{-1} and even up to 16.4 cm^2 V^{-1} s^{-1}.[8,9] Recently, we reported a series of novel naphthodithiophene-containing copolymers which were applied in organic photovoltaic devices (OPVs) with power conversion efficiencies up to 5.3%.[10] This result indicates that naphthodithiophene is a useful π-conjugated building block for organic semiconductors and motivated us to further introduce this planar core into other small-molecule and polymeric semiconductors.

The two important tetrabrominated naphthodithiophene intermediates **9** and **10** were derived from a common precursor, **8**, which was obtained by a milder bromination of **7** with *N*-bromosiccinimide (NBS) in 92% yield (Scheme 1).[11] Further bromination of **8** was then carried out with Br_2 as the brominating reagent. When the reaction was performed with a traditional acidic and polar solvent, AcOH,[12] the 3- and 8-positions of **8** were reactive and **9** was obtained. On the other hand, when a nonpolar solvent, CS_2, was employed, a different product was obtained which was identified as **10**. After optimization of reaction conditions, the precuror building blocks **9** and **10** could be obtained in moderate isolated yields.

Scheme 1. Synthesis of **9** and **10** by Bromination of Naphthodithiophene

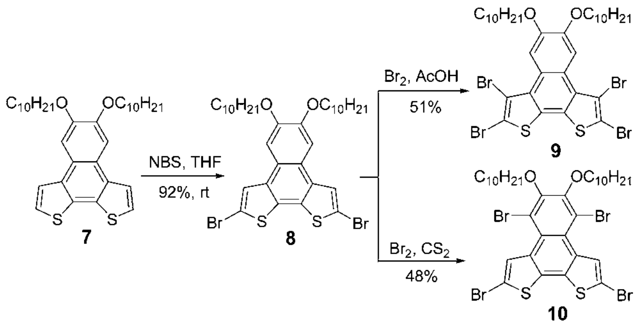

A palladium-catalyzed Suzuki coupling reaction of **9** with 5-hexylthiophene-2-boronic acid gave 7-aryl-ring intermediate **11**, which subsequently underwent $FeCl_3$ oxidative cyclization affording a highly soluble hexyl-substituted 10-fused-ring heteroacene **1** (Scheme 2). To prepare the unsubstituted analog, **9** was first cross-coupled with thiophene-2-boronic acid giving the intermediate **12**. However, direct $FeCl_3$ oxidative cyclization of **12** gave a very low yield of desired 10-fused-ring heteroacene **3**. Alternatively, NBS-bromination of **12** was carried out first and then followed by oxidative cyclization affording dibrominated 10-fused-ring heteroacene **2**. Debromination of **2** was carried out by bromide–lithium exchange followed by quenching with CH_3OH affording the desired product **3** in moderate isolated yield. On the other hand, **10** was used to synthesize a butterfly-shaped 8-fused-ring heteroacene. A Suzuki cross-coupling reaction of **10** with thiophene-2-boronic acid gave **14** in a moderate yield. Bromination of **14** by NBS afforded dibromo-substituted intermediate **15** in 97% isolated yield, which was then subjected to ring-closure oxidation with $FeCl_3$ giving dibrominated 8-fused-ring heteroacene **4**. Debromination of **4** with *n*-BuLi gave unsubstituted analog **6**. To improve the efficiency of the oxidation cyclization step, **14** was first converted to hexabromo-substituted intermediate **16** in quantitative yield by means of a large excess of NBS. $FeCl_3$ oxidative cyclization of **16** afforded hexabromo-substituted 8-fused-ring heteroacene **5** in an excellent yield. Following previously established debrominating steps, unsubstituted 8-fused-ring heteroacene **6** was also obtained.

The UV–vis absorption spectra of the fused heteroacenes **1**, **3**, and **6** in CH_2Cl_2 solution were next examined (Figure 1a and Table 1). Despite the identical π-conjugated skeleton, the absorption maximum of **1** is slightly red-shifted relative to that of **3** (Δ = 8 nm) which tallies with the effect of the terminal alkyl group in oligothiophenes.[13] Interestingly, **6** shows a dramatic red shift in the absorption spectrum with an absorption maximum peaking at 484 nm in CH_2Cl_2 as compared to those of **1** and **3**. This finding suggests that the π-conjugated electrons are more efficiently delocalized in **6** because **6** has a greater conjugated path than those of **1** and **3**. There is a pronounced difference in the absorption behavior of **1** and **3** in thin films (Figure 1b). The thin film of the compound **1** exhibits a red shift in the absorption spectrum, whereas **3** shows a blue shift in the absorption maximum in addition to spectra broadening as compared to those obtained from solution. The observed spectral shift in the thin films should probably result from different stacking arrangements in the thin film, which would lead to differences in charge carrier properties. The absorption spectrum of **6** also exhibits a large red shift and spectral broadening in the thin film, indicating a strong intermolecular interaction. The optical energy gaps of **1**, **3**, and **6** were calculated from

---

(7) (a) Feng, X.; Wu, J.; Ai, M.; Pisula, W.; Zhi, L.; Rabe, J.; Müllen, K. *Angew. Chem., Int. Ed.* **2007**, *46*, 3033. (b) Ma, C.; Mena-Osteritz, E.; Debaerdemaeker, T.; Wienk, M.; Bäuerle, P. *Angew. Chem., Int. Ed.* **2007**, *46*, 1679.

(8) (a) Takimiya, K.; Ebata, H.; Sakamoto, K.; Izawa, T.; Otsubo, T.; Kunugi, Y. *J. Am. Chem. Soc.* **2006**, *128*, 12604. (b) Ebata, H.; Izawa, T.; Miyazaki, E.; Takimiya, K.; Ikeda, M.; Kuwabara, H.; Yui, T. *J. Am. Chem. Soc.* **2007**, *129*, 15732. (c) Izawa, T.; Miyazaki, E.; Takimiya, K. *Adv. Mater.* **2008**, *20*, 3388.

(9) (a) Yamamoto, T.; Takimiya, K. *J. Am. Chem. Soc.* **2007**, *129*, 2224. (b) Minemawari, H.; Yamda, T.; Matsui, H.; Tsutsumi, J.; Haas, S.; Chiba, R.; Kumai, R.; Hasegawa, T. *Nature* **2011**, *475*, 364.

(10) Wang, B.; Tsang, S.; Zhang, W.; Tao, Y.; Wong, M. *Chem. Commun.* **2011**, 9471.

(11) Tovar, J.; Rose, A.; Swager, T. *J. Am. Chem. Soc.* **2002**, *124*, 7762.

(12) (a) Zhang, W.; Ng, G.; Tam, H.; Wong, M.; Zhu, F. *J. Polym. Sci., Part A: Polym. Chem.* **2011**, *49*, 1865. (b) Zhang, W.; Tse, S.; Lu, J.; Tao, Y.; Wong, M. *J. Mater. Chem.* **2010**, *20*, 2182.

(13) (a) Zhang, L.; Tan, L.; Wang, Z.; Hu, W.; Zhu., D. *Chem. Mater.* **2009**, *21*, 1993. (b) Gao, P.; Beckmann, D.; Tsao, H.; Feng, X.; Enkelmann, V.; Baumgarten, M.; Pisula, W.; Müllen, K. *Adv. Mater.* **2009**, *21*, 213.

Scheme 2. Synthetic Routes of Butterfly-Shaped Fused Heteroacenes **1**−**6**

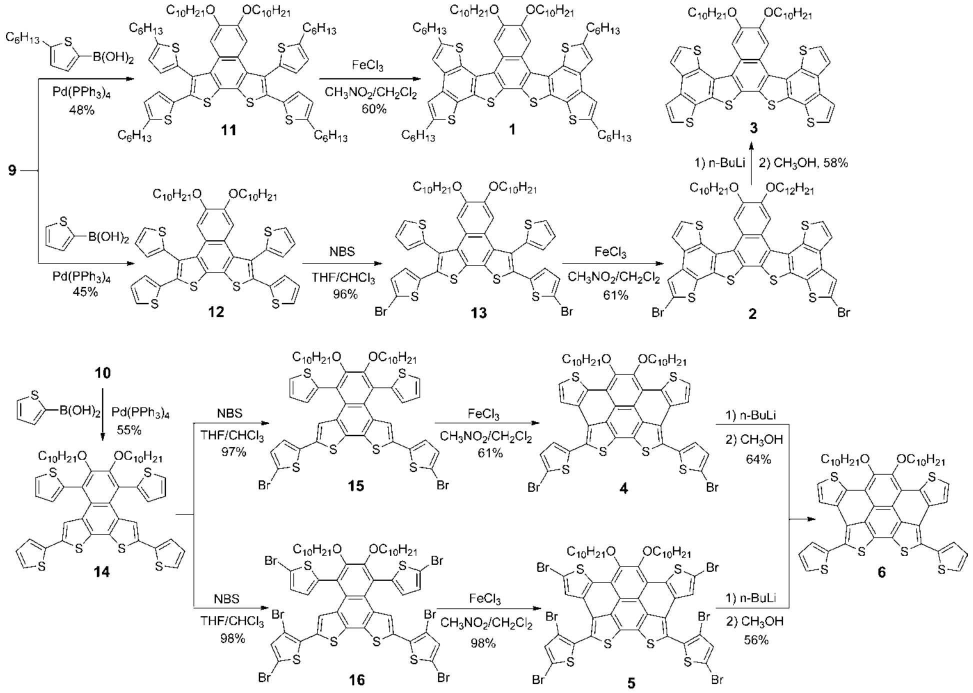

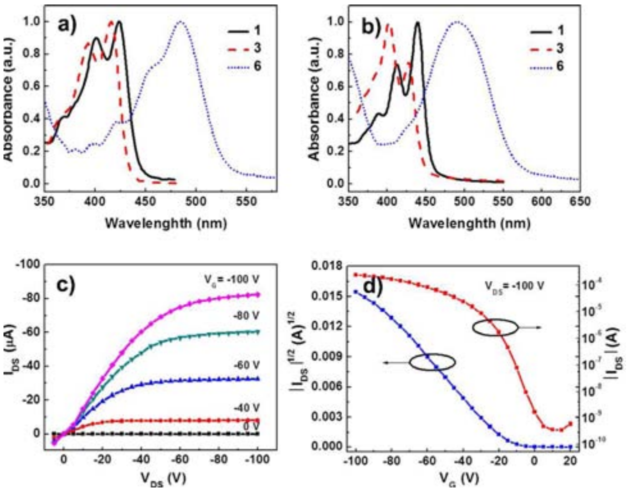

Figure 1. Absorption spectra of the butterfly shaped fused heteroacenes **1**, **3**, and **6** in (a) CH_2Cl_2 and (b) thin films; and the (c) output and (d) transfer characteristics of typical OFETs based on **1**.

the absorption onset of thin film to be 2.68, 2.76, and 2.17 eV, respectively.

To investigate the redox potentials of heteroacenes **1**, **3**, and **6**, cyclic voltammetry measurements were performed in dry CH_2Cl_2 (with 0.1 M $(n\text{-Bu})_4NPF_6$) using Ag/AgCl as a reference electrode (Figure S1 and Table 1). The three fused heteroacenes show very similar redox behavior with one quasi-reversible oxidation couple and one irreversible reduction wave. The onset oxidation potentials (E_{oxd}^{onset}) for **1**, **3**, and **6** are 0.86, 0.97, and 0.64 V, respectively, which correspond to the HOMO energy levels of −5.26, −5.37, and −5.04 eV using the equation $E_{HOMO} = -e(4.40 + E_{oxd}^{onset})$ eV. The HOMO values of **1** and **3** are lower than that of pentacene (−5.14 eV),[14] indicating that they have better stability than pentacene in electronic devices. The onset reduction potentials (E_{red}^{onset}) for **1**, **3**, and **6** are −1.36, −1.37, and −1.36 V, respectively, which correspond to the LUMO energy levels of −3.04, −3.03, and −3.04 eV using the equation $E_{LUMO} = -e(4.40 + E_{red}^{onset})$ eV. Thus, **1**, **3**, and **6** have similar LUMO energy levels.

Table 1. Summary of Physical Measurements of Heteroacenes **1**, **3**, and **6**

compd	λ_{max} (nm)[a]	E_{oxd}^{onset} (V)	E_{red}^{onset} (V)	E_{HOMO} (eV)[b]	E_{LUMO} (eV)[c]
1	424	0.86	−1.36	−5.26	−3.04
3	416	0.97	−1.37	−5.37	−3.03
6	484	0.64	−1.36	−5.04	−3.04

[a] Determined in CH_2Cl_2 solution. [b] $E_{HOMO} = -e(4.40 + E_{oxd}^{onset})$ eV. [c] $E_{HOMO} = -e(4.40 + E_{red}^{onset})$ eV.

OFET devices were fabricated by spin-coating the solutions of the fused heteroacenes **1**, **3**, and **6** on the octadecyltrichlorosilane (OTS)-modified SiO_2/Si substrates with a top-contact bottom-gate configuration. Gold was used

---

(14) Tang, M. L.; Okamoto, T.; Bao, Z. *J. Am. Chem. Soc.* **2006**, *128*, 16002.

as drain and source electrodes. The transistors based on these fused heteroacenes were found to exhibit typical *p*-type FET characteristics. Typical output and transfer characteristics of the OFET devices based on **1** are shown in Figure 1c and 1d. In the pristine film, the transistors exhibit a hole mobility up to 0.072 $cm^2\ V^{-1}\ s^{-1}$ with a current on/off ratio of 10^6. Reproducible results were obtained from different transistors. However, after annealing the thin films at 80 and 120 °C for 20 min, the device performance progressively decreased with increasing annealing temperature (Table 2). Such deterioration in device performance is attributed to the morphological change of the active layer by thermal annealing. On the other hand, the OFET devices based on **3** or **6** exhibit relatively low hole mobilities on the order of 10^{-4} and 10^{-5} $cm^2\ V^{-1}\ s^{-1}$ with a current on/off ratio of 10^4. Atomic force microscopy (AFM) was used to investigate the relationships between film morphology/crystallinity and device performance. The morphology of the **1** thin films undergoes pronounced change with increasing annealing temperatures (Figure S2). In the pristine film, the grains are small in size; however, the grain size grows larger and the grain boundaries become more apparent with increasing annealing temperature from rt to 80 and 120 °C, which results in a negative impact on the charge transport.

Table 2. FET Characteristics of the **1**-Based Devices Fabricated on OTS-Treated Si/SiO_2 Substrates under Different Annealing Temperatures (T_{sub})

T_{sub} (°C)	μ ($cm^2\ V^{-1}\ s^{-1}$)	I_{on}/I_{off}
pristine film	0.052–0.072	10^6
80	0.021–0.037	10^5
120	1.1×10^{-5}–3.9×10^{-5}	10^3

In summary, novel highly π-extended 10-fused-ring or 8-fused-ring butterfly-shaped heteroacenes **1**–**6** have been successfully synthesized based on two tetrabrominated naphthodithiophene intermediates. The as-fabricated OFET devices based on **1** exhibit a promising mobility up to 0.072 $cm^2\ V^{-1}\ s^{-1}$ with a current on/off ratio of 10^6 under an ambient atmosphere. These findings also highlight the potential of this 10-fused-ring heteroacene and the importance of the hexyl-substituents to achieve high charge mobility. Further optimization of these transistors and applications in OPVs is still in progress.

Acknowledgment. This research was financially supported by the National Science Foundation of China (20825208 and 21021091), the Major State Basic Research Development Program (2011CB808403, 2011CB932303), and Chinese Academy of Sciences. This work was also supported by a grant from the Hong Kong University Grants Committee, Areas of Excellence Scheme (AoE/P-03/08).

Supporting Information Available. Experimental procedures and full spectroscopic data for all new compounds. This material is available free of charge via the Internet at http://pubs.acs.org.

The authors declare no competing financial interest.